

## DIURNAL AND SEMIDIURNAL INTERNAL WAVES NEAR TWO HARBORS, SANTA CATALINA, CALIFORNIA

Craig Gelpi<sup>1</sup>

**ABSTRACT.**—Internal waves at both diurnal and semidiurnal frequencies are common on island slopes in the Southern California Bight (SCB). Amplitudes in both regimes are similar, although the phenomenology at the 2 frequencies is expected to be different since the bight is north of the critical latitude ( $30^\circ$ ), making diurnal modulations evanescent though semidiurnal waves can propagate. Understanding the driving forces for the internal waves may provide insight into vertical mixing in the bight. We used long-duration time series of ocean temperatures measured near the Wrigley Institute for Environmental Studies (WIES), Santa Catalina Island, to study highly resolved spectra and seasonal characteristics of internal waves. These characteristics were analyzed using available, sometimes nonconcurrent, ancillary data sets that include local tide and wind measurements. We conclude that the semidiurnal waves are driven by tides, whereas the diurnal waves are due to meteorological forcing.

**RESUMEN.**—Las olas internas en frecuencias diurnas y semidiurnas son comunes en las pendientes de las islas de la Bahía *Southern California Bight* (SCB). Las amplitudes de ambas frecuencias son similares, sin embargo se estima que la fenomenología en ambos casos debe ser diferente, debido a que la bahía se encuentra al norte de la latitud crítica ( $30^\circ$ ), lo cual determina que las modulaciones diurnas sean evanescentes y las olas semidiurnas se puedan propagar. El conocer cuáles son las fuerzas impulsoras de las olas internas ayudará a comprender la mezcla vertical que se produce en la bahía. Las series de tiempo prolongado de las temperaturas oceánicas que se miden cerca del Wrigley Institute of Environmental Studies (WIES), Isla Santa Catalina, se utilizan para estudiar los espectros de alta resolución y las características estacionales de las olas internas. Dichas características se analizan utilizando conjuntos de datos auxiliares, a veces no concurrentes, incluyendo las mediciones locales del viento y la marea. La conclusión es que las mareas impulsan las olas semidiurnas y que las olas diurnas se producen debido al forzamiento meteorológico.

Oscillations in the water column, or internal waves, are common on island slopes in the Southern California Bight (SCB) in both diurnal and semidiurnal frequency bands. Gelpi and Norris (2005) found internal waves to be ubiquitous in a survey of temperature data taken around Santa Catalina Island and in similar, though informal, analyses of temperature data provided by the Channel Islands National Park. The large specific heat capacity of water implies that large changes in temperature are due to advection of temperature gradients rather than local heating or cooling. Hence, temperature is a good tracer of water movements when these gradients exist, and rapid oscillations in temperature often signify internal waves.

Internal waves may have a significant impact on water mixing, and understanding this impact bears on many problems in physical and biological oceanography, as well as in island marine ecology. Gelpi and Norris (2008) demonstrated that vertical mixing in the upper 30 m in the inner SCB is much less than that in the

adjacent California Current. In the bight, vertical mixing is characterized by a vertical eddy diffusion coefficient of  $\sim 1 \text{ cm}^2 \cdot \text{s}^{-1}$ ; outside the bight in the California Current, diffusion is too rapid to measure with their techniques (i.e., the upper layers are well mixed). Understanding the physics that produces this value for the diffusion coefficient will provide insight into the water and nutrient flows of the bight. It may also help us discern mixing in the abyss, which has been inferred to have a similar value (e.g., Munk and Wunsch 1998).

Understanding island internal waves may provide insight into whether the forcing is a top-down mechanism (energy input at the surface that diffuses to depth) or a bottom-up one (energy input at depth that diffuses upward). Examples of the former are wind and surface waves that can mix the surface layers; an example of the latter are tidal interactions with seabed topography that may create mixing at the bottom. Each mechanism has ramifications to nutrient diffusion against the vertical

---

<sup>1</sup>Catalina Marine Society, 15954 Leadwell St., Lake Balboa, CA 91406. E-mail: craig@catalinamarinesociety.org

nutrient gradient. Each may also elucidate the contribution of topography to a possible island mass effect: that is, the increased productivity produced by the presence of the island.

Finally, understanding internal oscillations at diurnal and semidiurnal frequencies should prove useful for interpreting biologically relevant oscillations found in ocean chemistry measurements. Recently Frieder et al. (2012) reported dissolved oxygen and pH measurements from a kelp forest off La Jolla, California. They found that at 7 m the diurnal variation of these parameters was larger than the semidiurnal variation, though the simultaneously measured temperature and pressure exhibited larger semidiurnal changes than diurnal ones. These differences may indicate different driving mechanisms or complicated gradients that must be interpreted within the context of the physical oceanography. Dissolved oxygen and pH are now being measured at the same site where the temperature data reported in this paper were taken, and the results obtained will be used in interpreting modulations found in these quantities.

There have been many studies of internal waves in the SCB and in the adjacent California Current (Price et al. 1986, Rosenfeld 1988, 1990, Lerczak et al. 2001, 2003, Pidgeon and Winant 2005, Beckenbach and Terrill 2008, Noble et al. 2009, Nam and Send 2011, 2013). Both diurnal and semidiurnal waves have been observed even though the phenomenology at the 2 frequencies is expected to be different because the bight is north of the critical latitude for diurnal waves ( $30^\circ$ ). The critical latitude (Lerczak et al. 2001) is where the inertial frequency (Apel 1987) is equal to the diurnal frequency ( $1/24 \text{ h}^{-1}$  or  $0.04167 \text{ h}^{-1}$ ). For locations poleward of the critical latitude, diurnal modulations are damped by inertial responses, though semidiurnal waves can propagate. The inertial frequency for the latitude of the study area is  $0.04606 \text{ h}^{-1}$ .

Several explanations and models have been suggested to account for diurnal temperature modulations poleward of the critical latitude. These include currents modifying the effective inertial frequency (Lerczak et al. 2001), barotropic tides driving nonlinear or localized behavior (Beckenbach and Terrill 2008, Pidgeon and Winant 2005), meteorological heating and mixing (Price et al. 1986), and diurnal sea breezes pooling warm surface water

against the coast, as described by Kaplan et al. (2003).

Our goal is to understand the upper-ocean internal-wave modulations at Santa Catalina Island in order to ascertain the contribution of the modulations to vertical mixing in the Southern California Bight. This study differs from the others mentioned above in that the measurements are made near the island and its associated topographical and meteorological effects.

## METHODS

### Data Sets

Water-temperature data were collected by the Catalina Conservancy Divers (CCD) at its WIES site (Wrigley Institute for Environmental Studies,  $33.45^\circ \text{ N}$ ,  $118.48^\circ \text{ W}$ ) and a nearby National Oceanic and Atmospheric Administration (NOAA) buoy (46025,  $33.75^\circ \text{ N}$ ,  $119.08^\circ \text{ W}$ ). Mean-sea-level (MSL) data were collected from Los Angeles Outer Harbor Station (9410660,  $33.72^\circ \text{ N}$ ,  $118.27^\circ \text{ W}$ ). All sites were sampled hourly during the year 2000. WIES is located on the leeward side, near the island isthmus (Fig. 1), where there is a near-sea-level pass from the windward side (Catalina Harbor) to the leeward side (Two Harbors). Elsewhere, the 2 sides are separated by mountains approximately 300 m in height. Data collected at WIES for this study were measurements made on the bottom at 4 depths: 4.6 m, 9.1 m, 18.3 m, and 30.5 m. The local and island shelf slope where these instruments were sited are both  $\sim 10^\circ$ . The NOAA buoy recorded near-surface temperature at 0.5 m depth. (for greater detail on these data, see Gelpi and Norris [2008] and references therein). The year 2000 was chosen because few dropouts occurred in the CCD data during this interval among the 4 depths at WIES. Data gaps were filled with values interpolated from the nearest good samples. There were approximately 10 such repairs, each consisting of one or 2 missing measurements.

In addition to the data described above, we employed meteorological data provided by a weather station (sampled every 0.5 h) at WIES during the years 2006–2009 and by the NOAA buoy for the years 2000 and 2006–2009. The weather station was located within a few hundred meters of the thermographs. The data sets, their locations, data types, intervals of operation, and sampling are listed in Table 1. The locations

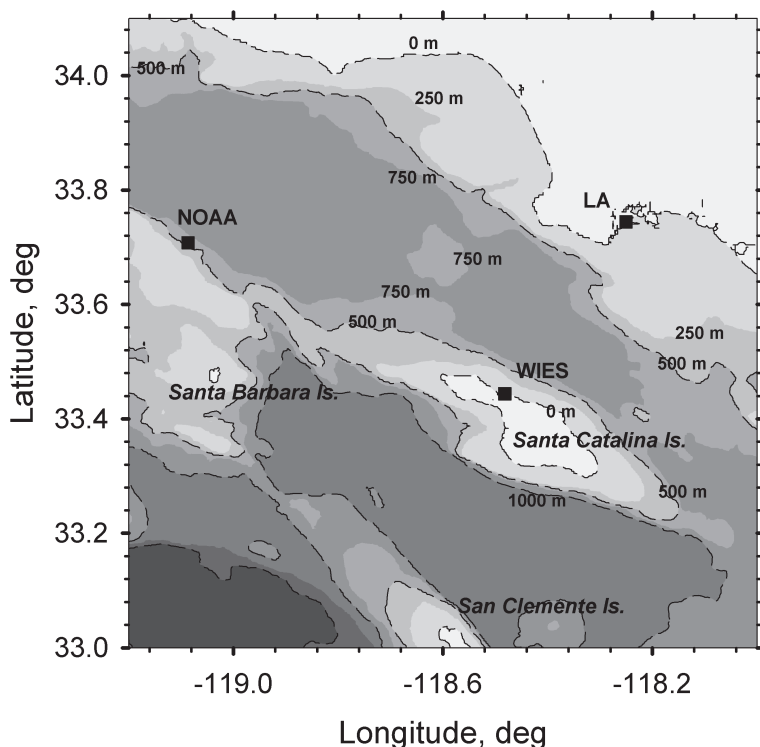


Fig. 1. Map showing data collection sites and bathymetry of the Southern California Bight.

TABLE 1. Data sets used to analyze internal waves near Two Harbors, Santa Catalina, California.

Organization/location	Instrument/Data	Time interval	Depth (m)	Sampling
NOAA Buoy 46025 33.75° N, 119.27° W	Wind	Year 2000, 2006–2009	Surface	Hourly
NOAA Buoy 46025 33.75° N, 119.27° W	Ocean temperature	Year 2000	0.5	Hourly
CCD 33.45° N, 118.48° W	Ocean temperature	01 Jan 2000: 31 Dec 2000	4.6, 9.1, 18.3, 30.5	Hourly
NOAA LA Station 9410660 33.72° N, 118.27° W	Water level	01 Jan 2000: 31 Dec 2000	—	Hourly
WIES 33.45° N, 118.48° W	Wind	2006–2009	—	0.5 hour

are shown also on the map in Fig. 1. The distances from WIES to the NOAA buoy and tide station are 65 km and 36 km, respectively. These ocean surface and tide measurements were the nearest available to the WIES study site.

#### Time Series Analysis

The time series of each data set was analyzed using both spectral and temporal methods.

Frequency decomposition via Fourier transform was performed to separate the effects of various driving mechanisms, such as lunar tides and meteorological effects, that operate at different frequencies. Data variance in small, discrete frequency bands (i.e., power spectral densities) were computed using conventional Fourier techniques as follows: the mean value of the time series was subtracted, the transform

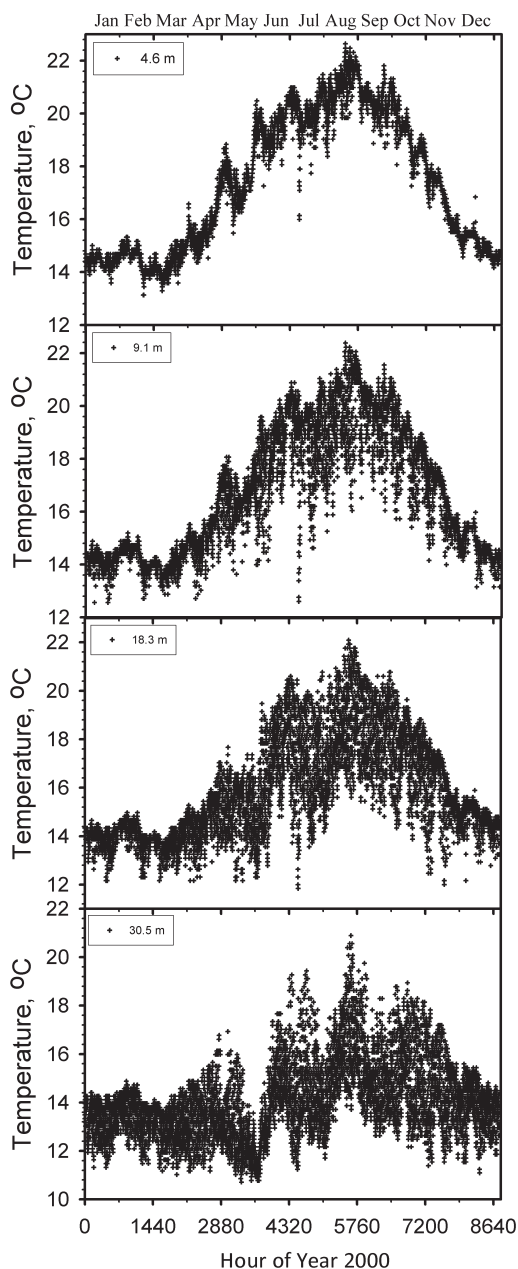


Fig. 2. Time series of WIES temperature data for each depth: 4.6 m, 9.1 m, 18.3 m, and 30.5 m.

computed and squared then scaled so the integral over frequency of the density estimates equals the variance of the original series. The series was not tapered so as to maintain the highest spectral resolution. Frequency units are kept in inverse hours to facilitate comparison

with the insolation period of 24 h, and power is displayed in decibels: that is, the base 10 logarithm of the power multiplied by 10. Spectral density was computed at 2 resolutions: high frequency resolution ( $0.000114 \text{ h}^{-1}$ ), achieved using the entire 8760-h series; and lower resolution ( $0.001389 \text{ h}^{-1}$ ), obtained using 720-h snippets. The power spectral densities computed from the snippets were concatenated to form spectrograms (i.e., power spectral density as a function of time of year). The latter analysis is designed to investigate the seasonal dependence of the power spectral density. Phase was computed as a function of frequency and time of year. Error bars to the phase value were computed using the coherence (Bendat and Piersol 1986) between the sinusoid and the corresponding power spectral density after smoothing by 3 bins.

Temporal analysis consisted of inspecting the average intraday modulation. This modulation was computed by subtracting the mean value for each 24-h interval and averaging the day-hour values over 90 days. The intraday modulation was computed for the winter and summer seasons. The advantage of examining the data using this technique is that diurnal, non-sinusoidal features are readily apparent, whereas a frequency analysis divides the features among its natural frequency and its harmonics. Temporal analysis is effective for understanding nonsinusoidal forcing mechanisms. Although similar analyses have been performed by Beckenbach and Terrill (2008) and Nam and Send (2011) with respect to the phase of diurnal surface tides, the analysis in this paper concerns the solar day.

## RESULTS

### High-Resolution Spectral Analysis

The temperature time series obtained from all the CCD thermographs at WIES for the year 2000 are plotted in Fig. 2. The time series indicate the typical seasonal response of upper-ocean temperate seas, with a  $7^\circ\text{C}$  warming from winter to late summer. There are also substantial modulations, particularly at depth where the modulation amplitude is as large as  $6^\circ\text{C}$ . Modulations are the result of surface water being transported to depth, as has been reported in Gelpi and Norris (2005). Note that the near-surface thermograph measured the least high-frequency modulation ( $>1/24 \text{ h}^{-1}$ ).

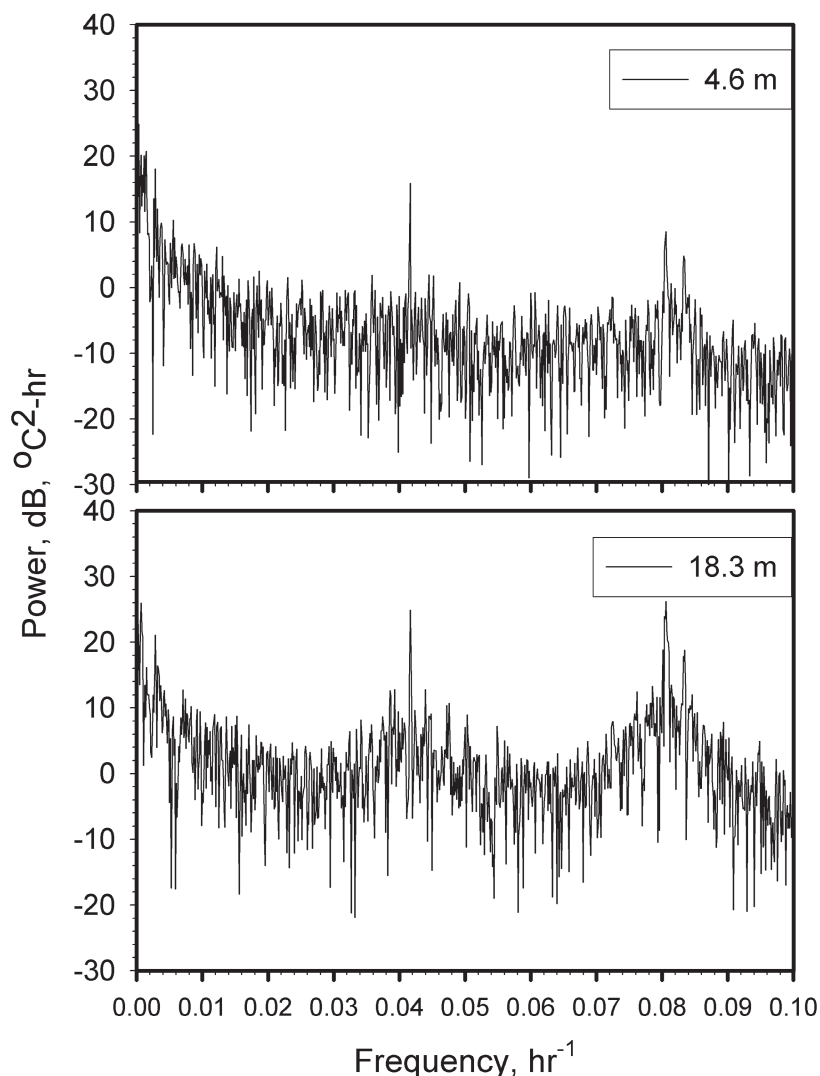


Fig. 3. High-resolution power spectral density for 4.6-m and 18.3-m depth data.

Figure 3 shows the power spectral densities obtained for the 4.6-m and 18.3-m data: the latter exhibiting a pattern similar to the 9.1-m and 30.5-m data. The spectra indicate substantial power in both the diurnal ( $\sim 1/24 \text{ h}^{-1}$ ) and semidiurnal ( $\sim 1/12 \text{ h}^{-1}$ ) bands. The peak power spectral densities computed from the 18.3-m depth data are larger than those obtained from the 4.6-m depth data. At 18.3-m depth, the largest power peak is in the semidiurnal regime; whereas, at 4.6 m, the largest peak is in the diurnal regime. Both the 9.1-m and 30.5-m data (not shown) have spectral densities similar in values to the 18.3-m data

and also have semidiurnal power greater than the diurnal power.

To investigate whether surface tides drive the internal tides, we compared peak frequencies in the power spectral density of the MSL found in Los Angeles Harbor and the 18.3-m WIES thermograph data (Fig. 4). To facilitate frequency comparisons, the power spectral densities are normalized by the highest power peak within the combined diurnal and semidiurnal bands. The frequency of the normalizing peak differed between the temperature and MSL spectra. An expanded view of the diurnal spectral regime is shown in Fig. 4A, where 3

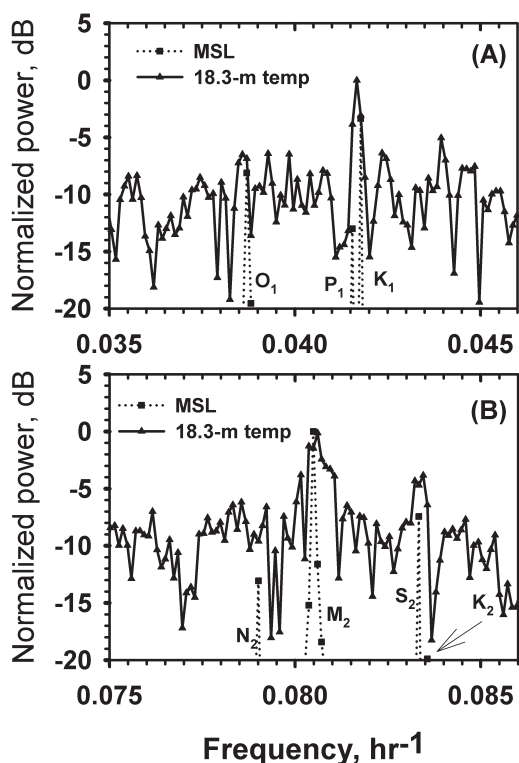


Fig. 4. Normalized 18.3-m and MSL spectra: A, diurnal regime; B, semidiurnal regime.

tidal frequencies are found in the MSL spectrum: the principle lunar ( $O_1$ ) at  $0.03873 \text{ h}^{-1}$ , the principle solar ( $P_1$ ) at  $0.04155 \text{ h}^{-1}$ , and the lunisolar ( $K_1$ ) at  $0.04178 \text{ h}^{-1}$ . All these power peaks extend many dB above the MSL noise level, which is substantially below the range plotted. The 2 lunar-related tides  $K_1$  and  $O_1$  have the largest power in MSL. In contrast, the diurnal temperature spectrum exhibits one peak above the background, which is exactly at  $0.04167 \text{ h}^{-1}$  or  $1/24 \text{ h}^{-1}$ , the insolation frequency which lies between the  $P_1$  and  $K_1$  tidal peaks. The peak is unambiguous, being  $\sim 10$  dB above the background. No temperature power is evident at the  $O_1$  frequency.

The semidiurnal regime is shown in Fig. 4B, and 4 peaks in the MSL spectrum are evident: lunar elliptic ( $N_2$ ),  $0.07900 \text{ h}^{-1}$ ; principle lunar ( $M_2$ ),  $0.08051 \text{ h}^{-1}$ ; principle solar ( $S_2$ ),  $0.08333 \text{ h}^{-1}$ ; and lunisolar ( $K_2$ ),  $0.08356 \text{ h}^{-1}$ . There are 2 complexes of peaks in the temperature spectrum centered at  $0.08062 \text{ h}^{-1}$  and at  $0.08333 \text{ h}^{-1}$ , roughly corresponding to the  $M_2$  spectral peak (lunar tidal) and the  $S_2$  solar

tidal. Lower-magnitude tidal peaks are not expected to be found in the temperature record if their effects scale with MSL power (e.g., the  $N_2$  peak would be below the temperature power spectral background, approximately  $-12$  dB on the relative scale).

#### Seasonal Spectra

The spectra in Figs. 3 and 4 are computed at the highest resolution in order to measure the spectral peaks precisely. However, seasonal dynamics in the power spectra are lost when all the data in the series are used in this manner. Seasonal dependence of the modulations were investigated by computing the spectra over shorter time intervals to create spectrograms. Spectrograms for the data gathered at each depth are shown in Fig. 5. There are prominent diurnal and semidiurnal bands in each panel, as well as harmonics of these frequencies. The largest power values are observed during the summer months. However, there is considerable difference between the 4.6-m data and the data for greater depths. Also note that the diurnal power is not large at the 9.1-m and 18.3-m depth data during the first 90 days of the year but is present in the 4.6-m and 30.5-m depth data.

In addition to the power, the phase lag relative to the beginning of the year in GMT (local midnight has a phase of  $120^\circ$  in this convention for the diurnal frequency) was computed for the CCD and buoy temperature and MSL data. The phases for the  $1/24 \text{ h}^{-1}$  bin are shown in Fig. 6A. The error bars are determined from the coherence and degrees of freedom. The coherence was high, averaging, for example, 0.8 for the 30.5-m data. The temperature phases are relatively constant throughout the year. The buoy and 4.6-m WIES temperatures are in phase during the winter, with an average value near  $0^\circ$  which corresponds to 1600 local time (LT). Temperatures at the 3 deeper depths at WIES are in phase with a value of  $\sim 135^\circ$ , corresponding to a time of maximum temperature near local midnight.

The MSL phase varies monotonically because the large tidal component  $K_1$  ( $0.04178 \text{ h}^{-1}$ ) is a discrete, narrowband feature that is offset from the center of the  $1/24 \text{ h}^{-1}$  frequency bin, thereby advancing the phase by the frequency offset ( $0.00011 \text{ h}^{-1}$ ) multiplied by the 720-h time increment between spectral calculations ( $30^\circ$ ). The lack of much variation in

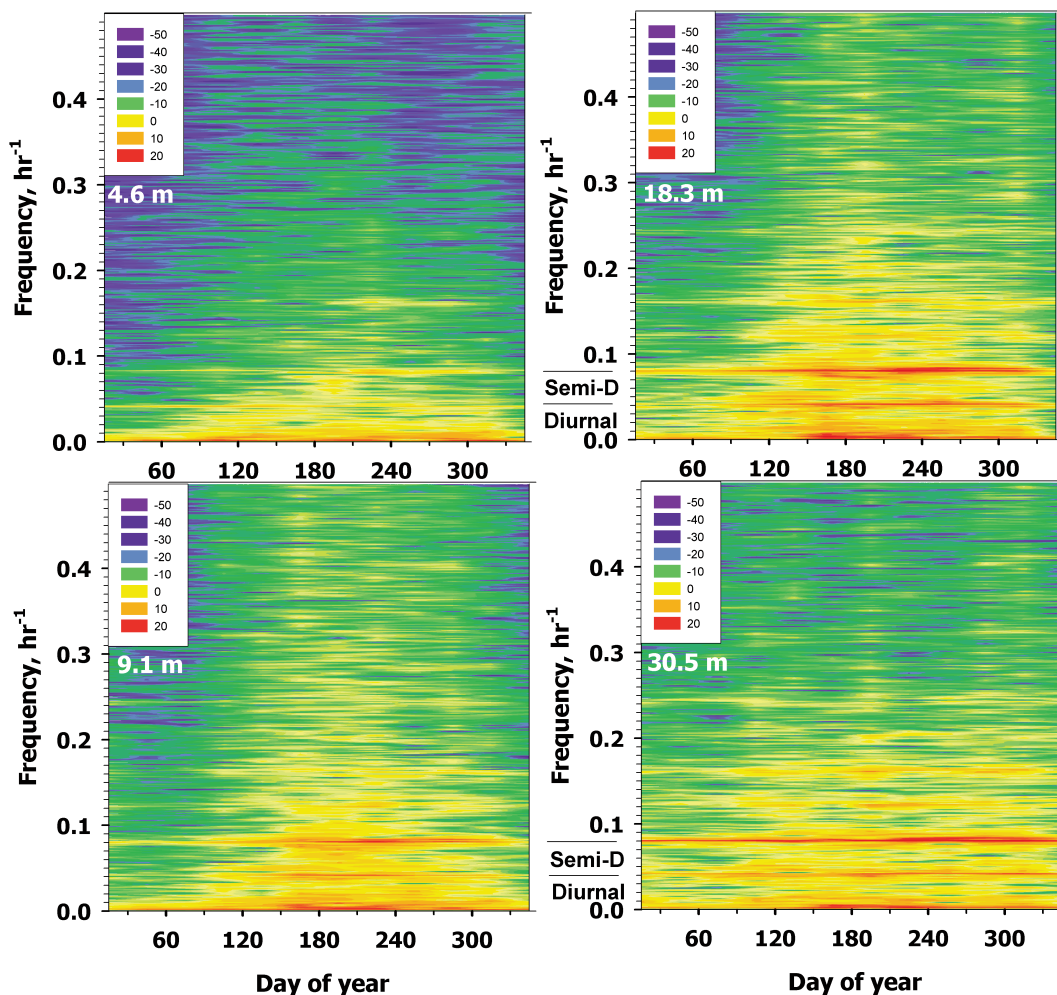


Fig. 5. Spectrograms computed from WIES data. Units are dB relative to °C<sup>2</sup>-h. The diurnal and semidiurnal frequencies positions are marked.

the phase of the diurnal temperature throughout the year indicates that the power is either uniformly spread over the spectral bin (contrary to the high-resolution measurements described above) or that it corresponds exactly to a period of 24 h.

The absolute phase for the semidiurnal frequency bin ( $1/12 \text{ h}^{-1}$ ) is plotted in Fig. 6B. The MSL phase averages  $139.8^\circ$ , corresponding to local times of 3.4 h before noon and midnight. NOAA uses a value of  $141.1^\circ$  for tidal prediction of this component at this location (<http://tide.sandcurrents.noaa.gov>). The difference between the published value and that obtained from our analysis of the tide data falls within the uncertainty of our phase measurement. Also,

the  $K_2$  component is within the semidiurnal frequency bin, with an offset of  $0.00023 \text{ h}^{-1}$ , which produces a semiannual modulation to the MSL phase. The 9.1-m, 18.3-m, and 30.5-m temperatures are all roughly in phase and vary between  $-30^\circ$  and  $150^\circ$  in a systematic fashion, though the  $K_2$  modulation is not evident as it is in the MSL data. The 9.1-m and 18.3-m data are considered to be temporally aliased at day 75 and day 105, as that maintains continuity with the other values (the phases of the 9.1-m and 18.3-m data are slightly greater than  $180^\circ$  for these days, but they are shown as negative values because the phase is forced to lie between  $180^\circ$  and  $-180^\circ$ ). The near-surface temperature phase at the buoy is

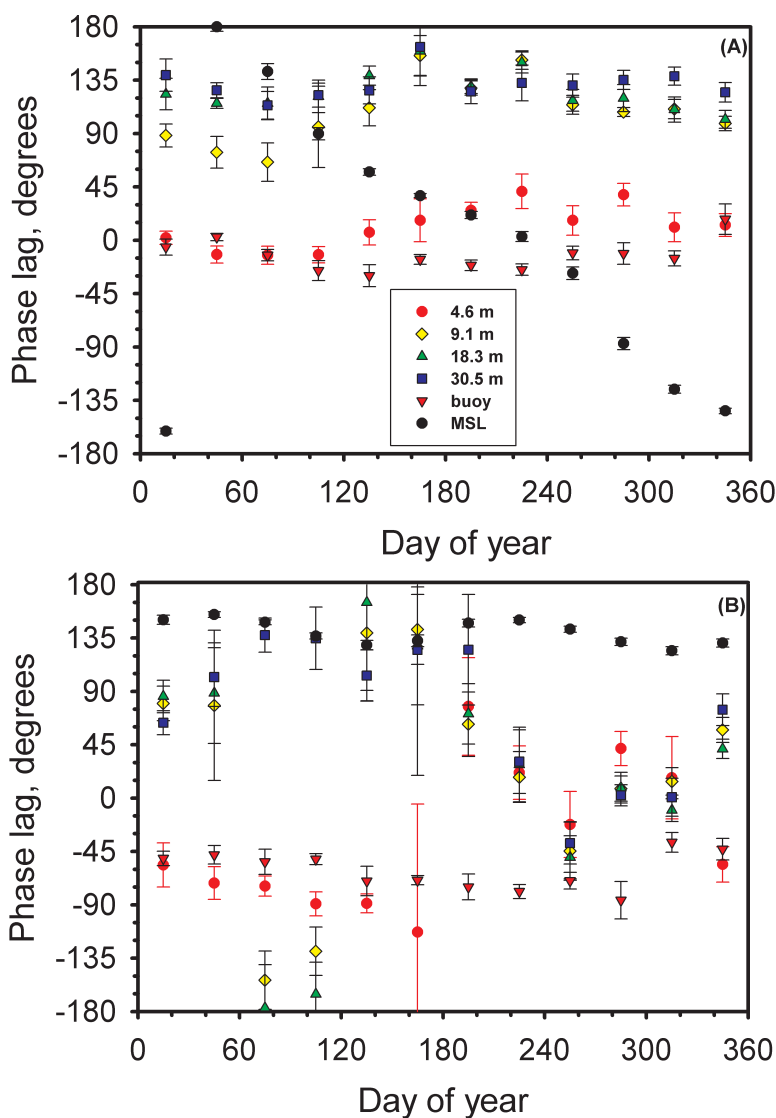


Fig. 6. Phases for the spectrograms shown in Fig. 5: **A**, frequency bin  $1/24 \text{ h}^{-1}$ ; **B**, frequency bin  $1/12 \text{ h}^{-1}$ .

nearly constant at  $-60^\circ$  (1400 LT). The 4.6-m temperature is in phase with the buoy temperature during winter and spring and in phase with the data from the deeper instrumentation for the rest of the year.

The wind forcing for the WIES and NOAA locations were very similar. Figure 7 depicts the spectrogram of the buoy's westerly wind for the year 2000. The power spectral densities for the east and north components (not shown) indicate that the wind was narrowband and originating predominantly from the west at both locations. Wind at the WIES site is

certainly influenced by the presence of the island, which is oriented in a northwest–southeast direction, and especially the isthmus, which is oriented in a northeast–southwest direction. The narrowband diurnal wind occurred all year. Other interesting features include the larger lower-frequency ( $<1/24 \text{ h}^{-1}$ ) wind events found during the winter when the marine temperature gradient collapses (Fig. 2).

#### Temporal Modulations

The spectrograms illustrate the Fourier decomposition of the signals as a function of time.

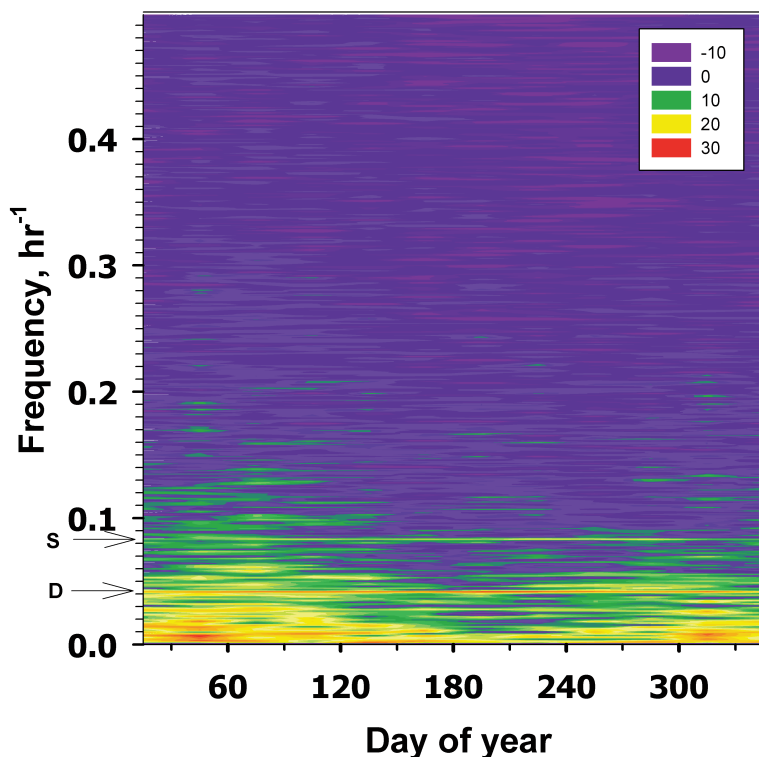


Fig. 7. Spectrogram of buoy westerly wind for year 2000. Units are dB relative to  $(\text{m/s})^2\text{-h}$ . Diurnal (D) and semidiurnal (S) frequency locations are marked.

Examining the average intraday modulation is also useful because dynamic behavior may be more closely identified with forcing mechanisms. The average intraday modulation of the WIES and buoy temperature data for the first 90 days of the year (winter) are shown in Fig. 8A and for the middle 90 days (summer) in Fig. 8B. These intervals are chosen to separate the seasonal dependence of the modulations found in the spectrograms of Fig. 5. During the winter (Fig. 8A), the 4.6-m and buoy temperatures vary almost identically, reaching a maximum at about 1500 LT with amplitude of  $0.2^\circ\text{C}$ . This time of temperature maximum does not agree exactly with the time computed from the phase (1600 LT) given in Fig. 7 because the intraday plot contains the sum of all harmonics. The 9.1-m and 18.3-m temperatures have a very different daily behavior compared to the 4.6-m temperature, changing little throughout the winter day. This behavior is consistent with the small power spectral density values found in Fig. 5 for these depths. Close examination does indicate a semidiurnal variation

consistent with diminished power found in the winter for these depths. In contrast, the 30.5-m temperature trace has maximums at midnight and 0700 LT and a deep minimum at 1300 LT that is approximately  $0.6^\circ\text{C}$  below the nighttime plateau. The 30.5-m minimum occurs near the time of temperature maximum for the near-surface and 4.6-m data, indicating upwelling at depth as the near surface is heated. The average temperature gradient for this time of year and at this depth is  $-0.04^\circ\text{m}^{-1}$  (Gelpi and Norris 2008), indicating that the isotherms were upwelled 15 m.

The variation becomes more complicated during the summer (Fig. 8B). Here, the near-surface buoy temperature has a larger modulation ( $\sim 0.5^\circ\text{C}$ ), and it occurs 2 h earlier than in the winter data. The deeper thermograph data (9.1 m, 18.3 m, and 30.5 m) clearly show the semidiurnal behavior, with much larger amplitude than found in Fig. 8A. The 4.6-m summer data are a mix of the characteristics of the near-surface data and the deeper data, but overall have much less modulation.

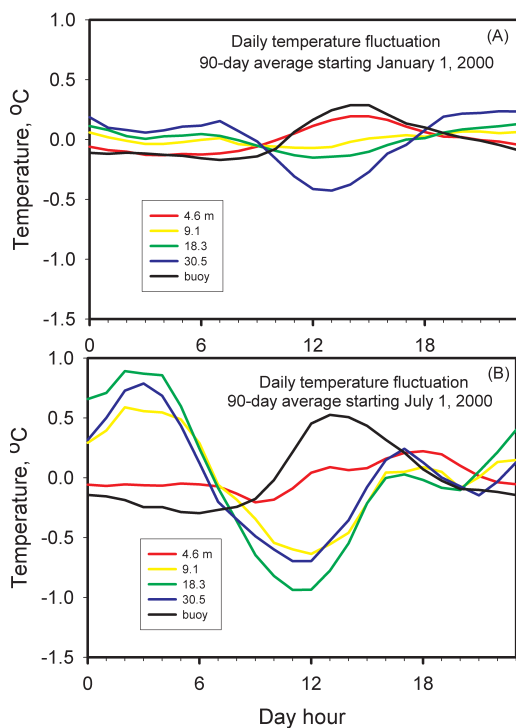


Fig. 8. Average intraday temperature modulation for WIES and buoy: **A**, winter; **B**, summer.

Although WIES and the buoy are located 65 km apart, the average intraday wind patterns are remarkably similar between them. Figure 9 shows the average intraday variation measured for 3 years (2006–2009) at the WIES weather station and the NOAA buoy. The intraday modulation is strongest at WIES, reaching almost  $9 \text{ m} \cdot \text{s}^{-1}$  out of the west at 1400 LT. This strong wind speed in the afternoon is well known anecdotally among scuba divers at WIES (including the author). The maximum wind at the buoy is smaller, with the peak occurring at 1600 LT. The north–south modulation is very small, with a minimum–maximum difference of  $2 \text{ m} \cdot \text{s}^{-1}$  and peaking between 1200 and 1300 LT for both sites. Thus the wind forcing is qualitatively the same at the 2 locations, though it peaks earlier in the day at WIES and is stronger there. Lerczak et al. (2001) reported on wind patterns measured at the Scripps Institution of Oceanography pier ( $32.87^\circ \text{N}$ ,  $117.26^\circ \text{W}$ ) during summer 1999. According to their measurements, the onshore westerly wind peaked at 1440 LT, with a value of  $1.7 \text{ m} \cdot \text{s}^{-1}$  (i.e., it had similar phase though much less velocity than the values applicable to WIES).

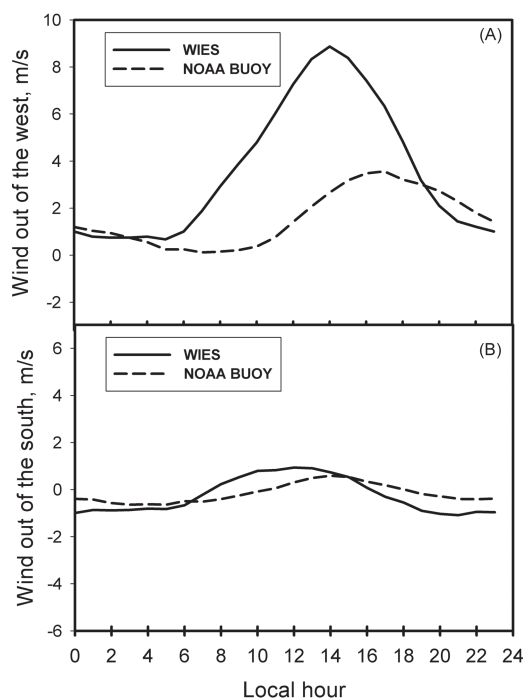


Fig. 9. Average intraday wind modulation for years 2006–2009: **A**, westerly wind; **B**, southerly wind.

#### SUMMARY OF RESULTS

Temperature modulations are found at the surface and all depths in both the diurnal and semidiurnal regimes and exhibit a complex phenomenology. The 2 frequency regimes differ in seasonal response, signal bandwidth, and correspondence to the barotropic tide, with the diurnal band having a narrow bandwidth at the insolation frequency and the semidiurnal band being broad with some power peaks at tidal frequencies. The 4.6-m data exhibit semidiurnal power predominantly during the summer months and diurnal power all year. The 18.3-m data show significant power all year in the semidiurnal band; but in the diurnal band, power is greatly diminished around March, day 60. The diurnal variations of the near-surface and 4.6-m temperatures are in phase and exhibit a maximum value at 1600 LT. The diurnal variations at the deeper thermographs are in phase with each other and have a temperature maximum at about local midnight. The semidiurnal surface temperature peaks between 0300 and 0400 LT and again between 1500 and 1600 LT. The semidiurnal phase at 4.6 m alternates

TABLE 2. Internal wave phenomenology, forcing, and rationale.

	Winter		Summer	
	Diurnal	Semidiurnal	Diurnal	Semidiurnal
SHALLOW, <5 M	Solar heating and wind mixing	Solar heating and wind mixing	Solar heating and wind mixing	Conventional buoyancy oscillations forced by tides
	In-phase relationship with near-surface buoy temperatures and insolation	Harmonic of diurnal waves	In-phase relationship with near-surface and insolation	Frequency corresponding to lunar tide and in-phase relationship with deeper waves
DEEP, >5 M	Wind-driven upwelling at 30.5 m Upwelling and solar heating cancellation at intermediate depths	Conventional buoyancy oscillations forced by tides	Wind-driven upwelling	Conventional buoyancy oscillations forced by tides
	Correspondence with diurnal wind and anti-correlated with insolation at 30.5 m	Frequency corresponding to lunar tide	Correspondence with diurnal wind and same absolute phase as found in winter	Frequency corresponding to lunar tide

between the surface temperature phase (summer) and those found at depth (winter). The wind is a narrowband frequency phenomenon; and at WIES, peaks at about 1400 LT. Although concurrent wind measurements and ocean temperature measurements are not available, by using the buoy wind measurements as a proxy for the island measurements, one finds westerly narrowband wind existed throughout the year 2000. The significance of narrow bandwidth is that it allows correlation with related phenomena.

#### DISCUSSION

In this section, the phenomenology described above are organized and assigned probable physical driving mechanisms. They are placed in context and contrasted with results from other similar studies performed on the nearby mainland. Finally, the significance of the results is discussed.

The analysis results above are divided into regimes of frequency, depth, and season. The frequency regimes are diurnal and semidiurnal. A depth of 5 m is used as the dividing point between near-surface (including the buoy temperature and 4.6-m thermograph data) and deeper thermograph data. Seasons are winter and summer, corresponding to relatively small and large stratification, respectively. The apparent forces can be divided into meteorological

and astronomical, with the former including direct solar heating and wind, whereas the latter is tidal. The significant forces for each regime are described below and are also organized into Table 2.

The deeper semidiurnal temperature response appears to be a tidally driven internal wave of large seasonal amplitude (with a displacement sometimes nearly equal to the depth of the water column). This measure is supported by the presence of lunar tidal frequencies in the response and the diminishing seasonal response when the temperature gradient is smallest, implying that these waves are vertical advectations of the temperature gradient. Observations of these waves are common (e.g., Baines 1986), and perhaps the amplitudes are enhanced by the seabed gradient, which is about  $10^\circ$  both locally and out to the island shelf (Fig. 1). These waves are not damped, as the semidiurnal frequency is above the inertial frequency.

The summer shallow semidiurnal fluctuations, at 4.6 m, appear to be a combination of solar heating and internal waves. The mixed-layer depth (i.e., the upper layer of small temperature gradient) may shoal during the summer as indicated by the temperature model for the inner SBC developed by Gelpi and Norris (2008). This situation would be conducive to internal wave activity being evident near the surface. Internal wave activity is supported by

the 4.6-m temperature data, which exhibited semidiurnal fluctuations with the same phase as the deeper thermograph data. These fluctuations are not expected at the buoy because internal wave amplitudes decrease to zero at the surface and the buoy is not adjacent to topography conducive to generating these waves. The summer and winter portions (1000 h each) of the year 2000 data set studied here were included in the Gelpi and Norris (2005) study, and the results presented here are consistent with the other 2 data sets taken during the summers and winters of 1998 and 1999. All of these data sets exhibit dichotomy in phase relationships as a function of depth and season (i.e., the semidiurnal modulation found at 4.6 m is in phase with the modulations at deeper depths during the summer and out of phase with them during the winter).

The winter shallow diurnal fluctuations are consistent with solar heating of the surface and simultaneous wind mixing to 5 m. This effect has been previously studied (Price et al. 1986) and is evidenced here by the near-surface buoy and 4.6-m thermograph temperature modulations being almost identical and having the same phase during most of the year. The semidiurnal shallow fluctuations are also narrow-band and are probably the result of harmonic distortion, as the mean daily fluctuation is not a sinusoid (Fig. 8).

Finally, the winter deep fluctuations have additional depth dependence in that there is little modulation at 9.1 m and 18.3 m, but a signal at 30.5 m. Interestingly, the deep-depth signal is out of phase with both the shallow-depth signal, the wind, and the insolation. This difference in phase suggests that the at-depth signal may be the result of upwelling produced by the wind. The diurnal wind has approximately the correct phase to transport surface water away from the island and to produce local upwelling as measured. This effect is similar to that described by Kaplan et al. (2003), the difference being that the diurnal breeze blows away from the shore at the WIES site and flows toward the shore at the site of the Kaplan et al. study. The effects of solar heating dominate near the surface but appear to be approximately balanced with upwelling at intermediate depths so that temperature signals are small at 9.1 m and 18.3 m. Another possible explanation for the small signal at intermediate depths is that collapse of stratification during

the winter has reduced the average seasonal temperature gradient there. Countering this seasonal trend is the simultaneous surface heating and upwelling and cooling at 30-m depth that adds a temperature gradient of  $-0.03^{\circ} \text{ m}^{-1}$  in the afternoon. Thus, competing effects are balanced at the intermediate depths.

Recent analyses of the diurnal internal tide found on the continental shelf off Huntington Beach northeast of the WIES study were conducted by Nam and Send (2011, 2013). At this location, diurnal wind is also present and is similar to, though less than, the wind at the WIES site. Additionally, the wind blows inshore at this location, whereas it blows offshore at WIES. However, the submarine topography is very different, with a slope of approximately  $0.5^{\circ}$  (much smaller than that at WIES). Diurnal modulations off Huntington Beach (Nam and Send 2011) appear to be phase locked with the barotropic or surface tide, rather than with diurnal meteorological drivers. Deep (cooler) water was found to intrude into the surf zone and then dissipate as the tide ebbed. This behavior was not noticed at WIES.

In subsequent work in the same area (Nam and Send 2013), diurnal oscillations driven by a sea/land breeze were reported. This report is partially consistent with our observations of water at depth (20 m) flowing opposite the breeze. Nam and Send attribute the diurnal oscillations to a resonant phenomenon where subinertial current shears can lower the effective inertial frequency to below the diurnal frequency (Lerczak et al. 2001). This mechanism does not appear to be present at WIES. Although current shear measurements are not available to confirm the model, diurnal modulations at depth occur throughout the year. However, the large-scale currents that would produce the shear are known to change with the season (Hickey 1993). Also, the phenomenon is not seen at intermediate depths—a fact not explained by shifts in the effective inertial frequency.

The diurnal upwelling found in the 30-m WIES data attributed to the diurnal wind is in contrast to the island's sheltering effects studied by Caldeira and Marchesiello (2002). They noted that the wind shadowing produced warmer sea surfaces which probably resulted in less mixing and nutrient availability. In contrast, the WIES site is not sheltered from the prevailing winds due to the near-sea-level pass

connecting Catalina Harbor and Two Harbors. Indeed, the pass may amplify the wind and subject the local area to higher winds than are found elsewhere, as noted above. The result is upwelling found in the deeper-depth temperature data and its implied transport of nutrients to shallower depths. This effect is probably local to WIES due to the vicinity of the pass.

#### CONCLUSION

Internal waves deduced from temperature data measured near Two Harbors, Santa Catalina Island, exhibited a complex behavior that includes variation at both diurnal and semidiurnal frequencies and a pronounced seasonal and depth dependence. During the winter, diurnal variations in surface and at-depth temperature were out of phase. Diurnal variations were driven by insolation near the surface (5 m) and by upwelling at 30-m depth—the latter probably produced by the diurnal wind directed offshore and lifting the isotherms by 15 m. Hence, both effects are driven by meteorological forces. During the winter, these effects appear to be approximately balanced at intermediate depths so that temperature signals are small at 9.1 m and 18.3 m.

During the summer, coherent water-column semidiurnal variations dominate, including near the surface, indicating that stratification was significant throughout the column. This stratification supported large amplitude waves that appear to be typical internal waves occurring over steep topography and driven by semidiurnal tides. Amplitudes were occasionally large enough to transport near-surface water to depth. Hence, there is significant vertical movement in the upper 30 m of the water column near WIES throughout the year.

#### ACKNOWLEDGMENTS

Karl Huggins of the University of Southern California provided the wind velocity data for WIES. The Santa Catalina Island marine-temperature data were provided by the Catalina Conservancy Divers, a group that supports the Catalina Island Conservancy; and Thomas Turney and John Turney were generous in securing and preparing the data sets. Sea-level data and buoy data were obtained from NOAA. This work profited from discussions with Karen Norris and was supported by the Catalina Marine Society.

#### LITERATURE CITED

- APEL, J.R. 1987. Principles of ocean physics. Academic Press, New York, NY.
- BAINES, P.G. 1986. Internal tides, internal waves and near-inertial motions. *In*: C.N.K. Mooers, editor, Baroclinic processes on continental shelves. American Geophysical Union, Washington, DC.
- BECKENBACH, E., AND E. TERRILL. 2008. Internal tides over abrupt topography in the Southern California Bight: observations of diurnal waves poleward of the critical latitude. *Journal of Geophysical Research: Oceans* (1978–2012), 113, C2, <http://dx.doi.org/10.1029/2006JC003905>
- BENDAT, J.S., AND A.G. PERSOL. 1986. Random data: analysis and measurement procedures. 2nd edition. John Wiley & Sons, New York, NY.
- CALDEIRA, R.M.A., AND P. MARCHESIELLO. 2002. Ocean response to wind shelter in the Southern California Bights. *Geophysical Research Letters* 29:13, <http://dx.doi.org/10.1028/2001GL014563>
- FRIEDER, C.A., S.H. NAM, T.R. MARTZ, AND L.A. LEVIN. 2012. High temporal and spatial variability of dissolved oxygen and pH in a nearshore California kelp forest. *Biogeosciences* 9:917–3930, <http://dx.doi.org/10.5194/bg-9-3917-2012>
- GELPI, C.G., AND K.E. NORRIS. 2005. Seasonal and high-frequency ocean temperature dynamics at Santa Catalina Island. Pages 461–471 *in* D.K. Garcelon and C.A. Schwemm, editors, Proceedings of the Sixth California Islands Symposium, Ventura, California, December 1–3, 2003. Technical Publication CHIS-05-01, National Park Service, Washington, DC.
- . 2008. Seasonal temperature dynamics of the upper ocean in the Southern California Bight. *Journal of Geophysical Research: Oceans* (1978–2012), Volume 113, Issue C4, <http://dx.doi.org/10.1029/2006JC003820>
- HICKEY, B.M. 1993. Physical Oceanography. *In*: M. Dailey, D. Reish, and J. Anderson, editors, Ecology of the Southern California Bight. University of California Press, Berkeley, CA.
- KAPLAN, D.M., L.L. LARGIER, S. NAVARRETE, R. GUINEZ, AND J.C. CASTILLA. 2003. Large diurnal temperature fluctuations in the nearshore water column. *Estuarine, Coastal and Shelf Science* 57:385–398.
- LERCZAK, J.A., M.C. HENDERSHOTT, AND C.D. WINANT. 2001. Observations and modeling of coastal internal waves driven by a diurnal sea breeze. *Journal of Geophysical Research: Oceans* (1978–2012), Volume 106, Issue C9, <http://dx.doi.org/10.1029/2001JC000811>
- LERCZAK, J.A., C.D. WINANT, AND M.C. HENDERSHOTT. 2003. Observations of the semidiurnal tide on the southern California slope and shelf. *Journal of Geophysical Research: Oceans* (1978–2012), Volume 108, Issue C3, <http://dx.doi.org/10.1029/2001JC001128>
- MUNK, W., AND C. WUNSCH. 1998. Abyssal recipes II: energetics of tidal and wind mixing. *Deep-Sea Research I*, 45, 1977–2010.
- NAM, S., AND U. SEND. 2011. Direct evidence of deep-water intrusions onto the continental shelf via surging internal tides. *Journal of Geophysical Research: Oceans* (1978–2012), Volume 116, Issue C05004, <http://dx.doi.org/10.1029/2010JC006692>
- . 2013. Resonant diurnal oscillations and mean alongshore flows driven by sea/land breeze forcing

- in the coastal Southern California Bight. *Journal of Physical Oceanography* 43:616–630.
- NOBLE, M., B. JONES, P. HAMILTON, J. XU, G. ROBERTSON, L. ROSENFELD, AND J. LARGIER. 2009. Cross-shelf transport into nearshore waters due to shoaling internal tides in San Pedro Bay, CA. *Continental Shelf Research* 29:1768–1785.
- PIDGEON, E.J., AND C.D. WINANT. 2005. Diurnal variability in currents and temperature on the continental shelf between central and southern California. *Journal of Geophysical Research: Oceans* (1978–2012), Volume 110, Issue C3, March 2005, <http://dx.doi.org/10.1029/2004JC002321>
- PRICE, J.F., R.A. WELLER, AND R. PINKEL. 1986. Diurnal cycling: observations and models of the upper ocean response to diurnal heating, cooling and wind mixing. *Journal of Geophysical Research: Oceans* (1978–2012), Volume 91, Issue C7, January 1986, Pages 8411–8427, <http://dx.doi.org/10.1029/JC091iC07p08411>
- ROSENFELD, L.K. 1988. Diurnal period wind stress and current fluctuations over the continental shelf off Northern California. *Journal of Geophysical Research: Oceans* (1978–2012), Volume 93, Issue C3, January 1988, Pages 2257–2276, <http://dx.doi.org/10.1029/JC093iC03p02257>
- \_\_\_\_\_. 1990. Baroclinic semidiurnal tidal currents over the continental shelf off Northern California. *Journal of Geophysical Research: Oceans* (1978–2012), Volume 95, Issue C12, January 1990, Pages 22153–22172, <http://dx.doi.org/10.1029/JC095iC12p22153>

*Received 9 February 2013*  
*Accepted 6 November 2013*  
*Early online 22 July 2014*